Journal of Computational Applied Mechanics 2024, 55 (1): 62-76

DOI: 10.22059/JCAMECH.2024.368866.909

RESEARCH PAPER

Investigating the Influence of Material Composition on Bending Analysis of Functionally Graded Beams Using a 2D Refined Theory

Mourad Chitour [a], Billel Rebai [b,*], Khelifa Mansouri [a,c], Faicel Khadraoui [a], Abdelak Berkia [a], Tidjani Messas[b]

[a] *Faculty of Sciences & Technology, Mechanic Eng Department, University Abbes Laghrour, Khenchela 40000, Algeria*

[b] *Faculty of Sciences & Technology, Civil Eng Department, University Abbes Laghrour, Khenchela 40000, Algeria*

[c] *Laboratory of Eng and Sciences of Advanced Materials (ISMA), Khenchela 40000, Algeria*

Abstract

This study attempts to shed light on the analysis of the static behavior of simply supported FG type property gradient material beams according to an original refined 2D shear deformation theory. Young's modulus is considered to vary gradually and continuously according to a power-law distribution in terms of volume fractions of the constituent materials. The equilibrium equations are obtained by applying the principle of virtual work. The governing equilibrium equations obtained are thus solved by using the analytical model developed here and Navier's solution technique for the case of a simply supported sandwich beam. Moreover, Using the numerical results of the non-dimensional stresses and displacements are calculated and compared with those obtained by other theories. Two studies are presented, comparative and parametric, the objective of which is the first to show the accuracy and efficiency of the theory used and the second to analyze the mechanical behavior of the different types of beams under the effect of different parameters. Namely boundary conditions, the material index , the thickness ratio and the type of beam.

Keywords: Mechanical behavior; beams; Property Gradient Materials; Principle of virtual work; Navier's solution.

1. Introduction

Functionally graded materials (FGMs) are a class of advanced composite materials that have continuous gradation in composition and structure over volume, resulting in corresponding changes in the properties of the material [1, 2]. The concept offers the potential to optimize material response or functionality by tailoring the microstructure. FGMs eliminate the stress concentrations and singularities that often occur in laminated composites by providing smooth transitions in material properties [3].

Beams are a common structural element analysed in FGM research. A wide variety of analytical and numerical

* Corresponding author. Tel.: +213-055-019-6631.
E-mail address: billel.rebai@univ-khenchela.dz

methods have been applied to study the behaviour of FGM beams under mechanical, thermal, and coupled thermo-mechanical loading conditions. Earlier works focused on developing analytical solutions and computational models for basic responses like bending, vibration and buckling of FGM beams based on Euler-Bernoulli beam theory [4-6]. More advanced beam theories accounting for shear deformation have been formulated and applied to improve accuracy for short, thick FGM beams [7-11]. Higher order and other refined beam theories continue to emerge in efforts to improve modelling fidelity[12-15] . The flexibility of FGMs has motivated study of advanced responses like geometrical and material nonlinear behaviour[16-18].

A variety of computational methods have been leveraged and developed alongside analytic solutions to model FGM beams, including finite element methods [19, 20], meshfree methods [21, 22], differential quadrature methods and others[23]. Benchmark solutions have been useful for validating new computational models and serve as reference solutions for code verification [24, 25]. Micromechanical models have also provided insight on relating the graded microstructure to global beam responses [26, 27]. FG sandwich beams have also been studied as they can provide enhanced stiffness and fracture toughness compared to traditional sandwich composites [28, 29].

Additional areas of active research include dynamic analysis of FGM beams [30], stability behaviour [31], formulation of theories accounting for additional effects like porosity [32]. Beams with variable thickness and other nonuniform geometries have also been explored [33-38]. Over-all, FGM beams remain a topic of significant research interest across the mechanics, materials and structures communities given the potential for tailoring gradation patterns and enabling advanced responses [39, 40].

Recent research has explored the dynamic stability and vibration characteristics of nanocomposite structures for aerospace and civil engineering applications. Advanced modeling techniques have been employed to capture the multiscale effects in these nanostructures.

The exploration the impact of CNT distributions near surfaces on the dynamic stability of functionally graded viscoelastic plates, revealing an expanded stability region [39, 40]. Another investigation focused on optimizing the dynamic buckling of aircraft shells using CNT nanocomposites, resulting in increased frequency and stability. A separate study utilized nonlocal strain gradient theory to analyze the buckling of carbon nanocones under magnetic and thermal loads, demonstrating improved stability with higher gradient parameters [41-46]

In the context of civil structures, an investigation was conducted to theoretically analyze wave propagation in porous sandwich beams with nanocomposite cores. The study revealed that increasing the volume fraction of nanoplatelets led to enhanced wave characteristics. Another examination focused on the fluid-structure interaction of pipes reinforced with silica nanoparticles, resulting in higher frequencies and critical velocity with increased nanoparticle concentration. Additionally, concrete pipes reinforced with nanofibers were analyzed under seismic loading, demonstrating a reduction in dynamic deflection [46-50].

Conical shells experienced reduced stability regions due to the influence of temperature and moisture. The study investigated the hygrothermal effects on defective graphene sheets. Additionally, an analysis of piezoelectric nanocomposite beams revealed the impact of agglomeration on stability. The low-velocity impact response of conical shells was also evaluated [9, 10, 51, 52].

This study comprises two integral components: a comparative study and a parametric study, each serving distinct purposes. The primary goal of the comparative study is to underscore the precision and efficacy of the theoretical framework employed in this investigation relative to alternative theories found in the literature. Conversely, the parametric study is designed to scrutinize the mechanical behavior of diverse Functionally Graded (FG) beams, taking into account a range of influential parameters. These parameters encompass the material index (k), which governs the power-law distribution of Young's modulus, the thickness ratio (a/h) dictating the geometric aspects of the beams, and the specific type of beam itself. Exploring the intricate interplay of these parameters, including how boundary conditions such as simply supported (SS), clamped-clamped (CC), and clamped-free (CF) affect the mechanical responses, yields valuable insights into the nuanced behaviors exhibited by FG beams under diverse constraints.

2. Functionally graded beam geometry

Fig 1 depicts a beam with length L, width b, and thickness h, which is referred to as a functionally graded beam. The beam is composed of face layers, where each layer is made up of an isotropic material that transition into a functionally graded material.

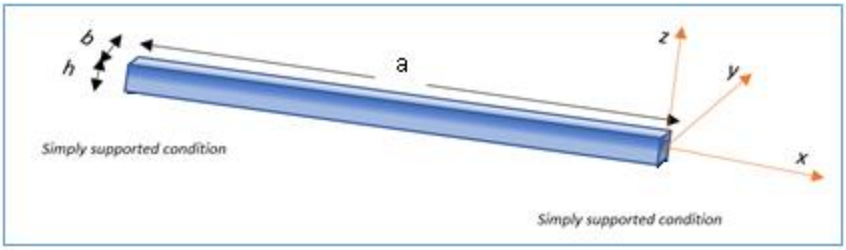

Fig 1: Geometry and coordinates of the FG beam.

The FG beam exhibits material properties, such as Young's modulus (E) and mass density (q) that undergo smooth variations solely in the z direction. These variations can be accurately described using the rule of mixture.

$$P(z) = P_c V_c + P_m V_m \qquad -\frac{h}{2} \le z \le \frac{h}{2} \tag{1}$$

The rule of mixture considers the proprieties of ceramic (P_c) and metal (P_m), as well as their respective volume fractions (V_c and V_m), and is mathematically expressed as follows:

$$V_c + V_m = 1 \tag{2}$$

To determine the volume fraction V_c, the profile is assumed to follow various simple power laws. The following expressions represent different types of profiles for the volume fraction V_c: linear, quadratic, cubic, and inverse quadratic.

$$\mathrm{V_c} = \begin{cases} \left(\frac{1}{2}+\frac{\mathrm{z}}{\mathrm{h}}\right) & \text{Linear} \\ \left(\frac{1}{2}+\frac{\mathrm{z}}{\mathrm{h}}\right)^2 & \text{Quadratic} \\ 3\left(\frac{1}{2}+\frac{\mathrm{z}}{\mathrm{h}}\right)^2 - 2\left(\frac{1}{2}+\frac{\mathrm{z}}{\mathrm{h}}\right)^3 & \text{Cubic} \\ 1-\left(\frac{1}{2}-\frac{\mathrm{z}}{\mathrm{h}}\right)^2 & \text{Inversequadratic} \end{cases} \tag{3}$$

3. Governing equations

In this study, we focus on investigating the displacement model of FG beams. We utilize a high-order shear strain theory, commonly known as the refined theory, to represent the model. The displacement model can be described by the following equation:

$$\begin{aligned} u(x,z) &= u_0(x) - z\,\frac{\partial w_b(x)}{\partial x} - f(z)\,\frac{\partial w_s(x)}{\partial x} \\ w(x,z) &= w_b(x) + w_s(x) \end{aligned} \tag{4}$$

Within the displacement model, wb represents the bending component, while ws represents the shearing component. These components describe the transverse displacement at a specific point situated on the median plane of the beam. To capture the shear deformation across the beam's thickness, a shape function, denoted as *f(z)*, is introduced. The specific form of the shape function *f(z)* is given by M. Chitour et al [32, 53]:

$$f(z) = \left(3/25\right)\pi z\left(\pi - \sqrt[3]{0.135}\cosh\left(\pi z/h\right)\right) \tag{5}$$

The strains are expressed as follows:

$$\varepsilon_x = \varepsilon_x^0 + z k_x^1 + f(z) k_x^2 \tag{6}$$

$$\gamma_{xz} = \left(1 - \frac{\partial f(z)}{\partial z}\right)\gamma_{xz}^{\grave{a}} = g(z)\gamma_{xz}^0 \tag{7}$$

Where: $g(z) = \left(1 - \frac{\partial f(z)}{\partial z}\right)$ is the shape functions of transverse shear deformations.

And

$$\varepsilon_x^0 = \frac{\partial u_0}{\partial x}, k_x^1 = -\frac{\partial^2 w_b}{\partial^2 x}, k_x^2 = -\frac{\partial^2 w_s}{\partial^2 x}, \gamma_{xz}^0 = -\frac{\partial w_s}{\partial x} \tag{8}$$

The linear constitutive relations of a FG beam can be expressed as:

$$\begin{Bmatrix} \sigma_{xx} \\ \tau_{xz} \end{Bmatrix} = \begin{bmatrix} C_{11} & 0 \\ 0 & C_{55} \end{bmatrix} \begin{Bmatrix} \varepsilon_{xx} \\ \gamma_{xz} \end{Bmatrix} \tag{9}$$

Where:

$$C_{11} = E(z), C_{55} = \frac{E(z)}{2(1+\nu)} \tag{10}$$

4. Equilibrium equations

The equations of equilibrium are obtained by applying the principle of virtual displacements. They can be formulated as follows:

$$\delta V_{tot} = \int_V \left[\sigma_{xx}\delta\varepsilon_{xx} + \tau_{xz}\delta\gamma_{xz}\right]dV - \int_\Omega q\,\delta w(x)\,d\Omega = 0 \tag{11}$$

The variation of the deformation energy of the (FG) beam can be defined as follows:

$$\mathrm{dU} = \int_0^1 \left(N_x \frac{\partial u_0}{\partial x} - M_b \frac{\partial^2 w_b}{\partial^2 x} - M_s \frac{\partial^2 w_s}{\partial^2 x} + Q_{xz} \frac{\partial w_s}{\partial x} \right) dx \tag{12}$$

The variation of the potential energy caused by the applied transverse load *q* on the FG beam is given by:

$$\delta V = -\int_A q\,\delta w(x)\,dx = \int_A q\,\delta\left(w_b(x) + w_s(x)_z\right) \tag{13}$$

By substituting the expressions of δU and δV from equations (13) and (12) into equation (11) and integrating throughout the thickness of the beam, the equilibrium equations of the FG beam can be expressed as follows:

$$\delta u_0 : \frac{\partial N_x}{\partial x} = 0, \delta w_b : \frac{\partial^2 M_b}{\partial x^2} + q = 0, \delta w_s : \frac{\partial^2 M_s}{\partial x^2} + \frac{\partial Q_{xz}}{\partial x} + q = 0$$

(14)

In these equations, the stress and moment resultants N_x , M_b , M_s *and* Q_{xz} are defined as follows:

$$N_x = \int_A \sigma_{xx} dz, \qquad M_b = \int_A \sigma_{xx} z dz,$$

$$M_s = \int_A \sigma_{xx} f(z)\, dz, \quad Q_{xz} = \int_A \tau_{xz} g(z) dz, \tag{15}$$

$$\begin{aligned} N &= L_1 \frac{\partial u}{\partial x} - L_2 \frac{\partial^2 w_b}{\partial x^2} - L_3 \frac{\partial^2 w_s}{\partial x^2} \\ M_b &= L_2 \frac{\partial u}{\partial x} - L_5 \frac{\partial^2 w_b}{\partial x^2} - L_6 \frac{\partial^2 w_s}{\partial x^2} \\ M_S &= L_3 \frac{\partial u}{\partial x} - L_6 \frac{\partial^2 w_b}{\partial x^2} - L_7 \frac{\partial^2 w_s}{\partial x^2} \\ Q_{xz} &= L_4 \frac{\partial w_S}{\partial x} \end{aligned} \tag{16}$$

With

$$\begin{aligned} L_1 &= \int_A C_{11} dA & L_5 &= \int_A z^2 C_{11} dA \\ L_2 &= \int_A z C_{11} dA & L_6 &= \int_A z f(z) C_{11} dA \\ L_3 &= \int_A f(z) C_{11} dA & L_7 &= \int_A f^2(z) C_{11} dA \\ L_4 &= \int_A g^2(z) C_{55} dA \end{aligned} \tag{17}$$

5. Analytical solutions

To solve the equilibrium equations, an analytical approach is employed utilizing the Navier solution. This approach allows for the derivation of analytical solutions specifically for a simply supported beam. By applying the Navier solution, it is determined that the solution can be expressed in the following form:

$$\begin{aligned} u(x) &= \sum_{m=1}^{\infty} U_n \cos(\lambda x) \\ w_b(x) &= \sum_{m=1}^{\infty} V_b \sin(\lambda x) \\ w_s(x) &= \sum_{m=1}^{\infty} W_s \sin(\lambda x) \end{aligned} \tag{18}$$

Where:

$\lambda = m\pi/L$, (U_n, V_b, W_s) are the unknown displacement coefficients.

The transverse load q is expanded in the Fourier series as well. The load amplitude q_n is determined using the calculations presented in:

$$q_n = \frac{2}{a} \int_0^a q(x) \sin(\lambda x) dx \tag{19}$$

q_n is given for a uniform charge:

$$q_n = \frac{4q_0}{m\pi} (m = 1,3,5,...)$$

(20)

$$\begin{Bmatrix} S_{11} & S_{12} & S_{13} \\ S_{21} & S_{22} & S_{23} \\ S_{13} & S_{23} & S_{33} \end{Bmatrix} \begin{Bmatrix} U_n \\ V_b \\ W_s \end{Bmatrix} = \begin{Bmatrix} 0 \\ q_n \\ q_n \end{Bmatrix} \tag{21}$$

With:

$$S_{11} = -L_1\lambda^2, S_{12} = L_2\lambda^3, S_{13} = L_3\lambda^3, S_{22} = -L_5\lambda^4, S_{23} = -L_6\lambda^4,$$
$$S_{33} = -A_4\lambda^2 - L_7\lambda^4, S_{21} = S_{12}, S_{31} = S_{13}, S_{32} = S_{23} \tag{22}$$

6. Results and discussion

In this section, the bending behavior of FG beams is investigated using Navier solutions. The analysis involves considering various theories and calculating the displacements and stresses of beams made with FG materials. The FG beams are composed of aluminum as the metal constituent (Al: E_m = 70 GPa, v_m = 0.3) and alumina as the ceramic constituent (Al_2O_3: E_c = 380 GPa, v_c = 0.3). Two raport ratios, l/h = 5 and 20, are examined. To facilitate the analysis, the vertical displacement of the beams under a uniformly distributed load q is expressed in non-dimensional terms. This allows for a more convenient comparison and understanding of the results.

$$\bar{w} = 100\frac{E_m h^3}{q_0 a^4} w\left(\frac{a}{2}\right), \bar{\sigma}_{xx} = \frac{h}{q_0 a}\sigma_{xx}\left(\frac{a}{2},\frac{h}{2}\right),$$
$$\bar{u} = 100\frac{E_m h^3}{q_0 a^4} u\left(0,-\frac{h}{2}\right), \bar{\tau}_{xz} = \frac{h}{q_0 a}\tau_{xz}\left(0,0\right). \tag{23}$$

6.1. Validation and accuracy

This section presents a numerical comparative study on the deflection, displacements and stress response of FG beams subjected to a uniform load. The non-dimensional results obtained are compared to existing analytical solutions from the literature to verify the accuracy of the present approach.

Table 1: Non-dimensional deflections and stresses of FG beams under uniform load *(a/h=5)*.

k	Method	$\bar{w}$	$\bar{u}$	$\bar{\sigma}_{xx}$	$\bar{\tau}_{xz}$
0	Li et al. [32, 53]	3.1657	0.9402	3.8020	0.7500
	Latifa et al. [32, 53]	3.1651	0.9406	3.8043	0.7489
	Vo, T.P et al. [32, 53]	3.1654	/	3.8020	0.7332
	Present	**3.1643**	**0.9375**	**3.7954**	**0.7333**
1	Li et al. [32, 53]	6.2599	2.3045	5.8837	0.7500
	Latifa et al. [32, 53]	6.2590	2.3052	5.8875	0.7489
	Vo, T.P et al. [32, 53]	6.2594	/	5.8836	0.7332
	Present	**6.2576**	**2.2999**	**5.8725**	**0.7326**
2	Li et al. [32, 53]	8.0602	3.1134	6.8812	0.6787
	Latifa et al. [32, 53]	8.0683	3.1146	6.8878	0.6870
	Vo, T.P et al. [32, 53]	8.0677	/	6.8826	0.6706
	Present	**8.0622**	**3.1082**	**6.8680**	**0.6700**
5	Li et al. [32, 53]	9.7802	3.7089	8.1030	0.5790
	Latifa et al. [32, 53]	9.8345	3.7128	8.1187	0.6084
	Vo, T.P et al. [32, 53]	9.8281	/	8.1106	0.5905
	Present	**9.8058**	**3.7020**	**8.0880**	**0.5902**
	Li et al. [32, 53]	10.8979	3.8860	9.7063	0.6436

10	Latifa et al. [32, 53]	10.9413	3.8898	9.7203	0.6640
	Vo, T.P et al. [32, 53]	10.9381	/	9.7122	0.6467
	Present	**10.9200**	**3.8764**	**9.6883**	**0.6458**

Table 2: Non-dimensional deflections and stresses of FG beams under uniform load (*a/h=20*).

k	Method	$\overline{w}$	$\overline{u}$	$\overline{\sigma}_{xx}$	$\overline{\tau}_{xz}$
0	Li et al. [32, 53]	2.8962	0.2306	15.0130	0.7500
	Latifa et al. [32, 53]	2.8962	0.2305	15.0136	0.7625
	Vo, T.P et al. [32, 53]	2.8962	/	15.0129	0.7451
	Present	2.8962	0.2305	15.0112	0.7455
1	Li et al. [32, 53]	5.8049	0.5686	23.2054	0.7500
	Latifa et al. [32, 53]	5.8049	0.5685	23.2063	0.7625
	Vo, T.P et al. [32, 53]	5.8049	/	23.2053	0.7451
	Present	5.8048	0.5685	23.2029	0.7435
2	Li et al. [32, 53]	7.4415	0.7691	27.0989	0.6787
	Latifa et al. [32, 53]	7.4421	0.7691	27.1005	0.7005
	Vo, T.P et al. [32, 53]	7.4421	/	27.0991	0.6824
	Present	7.4419	0.7690	27.0962	0.6815
5	Li et al. [32, 53]	8.8151	0.9133	31.8112	0.5790
	Latifa et al. [32, 53]	8.8186	0.9134	31.8151	0.6218
	Vo, T.P et al. [32, 53]	8.8182	/	31.8130	0.6023
	Present	8.8175	0.9132	31.8077	0.6015
10	Li et al. [32, 53]	9.6879	0.9536	38.1372	0.6436
	Latifa et al. [32, 53]	9.6907	0.9537	38.1408	0.6788
	Vo, T.P et al. [32, 53]	9.6905	/	38.1385	0.6596
	Present	9.6900	0.9535	38.1328	0.6590

Table 1-2 presents the non-dimensional numerical results for the deflection, vertical displacements, axial stress, and shear stress of an FG beam under a uniform load. The results are obtained for various values of the material index k, while simultaneously varying the beam's *a/h* ratio. The obtained results are compared with those obtained in literature using analytical methods.

Overall, the obtained results show a similarity with the results from all the compared theories in the relevant section. In other words, there is consistency between the results obtained in this study and the existing theories, with no significant discrepancies observed.

6.2. Parametric study

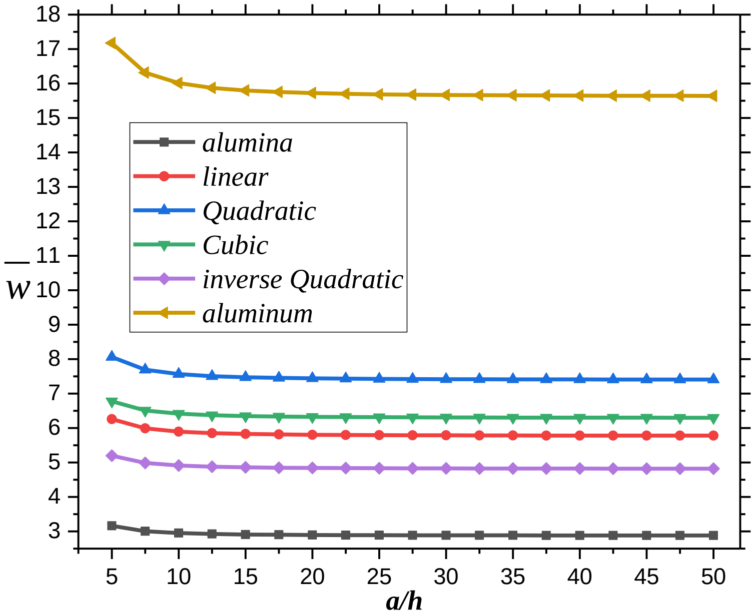

Fig 2 : Non-dimensional the center deflection change ($\bar{w}$) for the metal, ceramic and FGM beams versus side-to-thickness ratio (a/h) with deferent volume-fraction Vc.

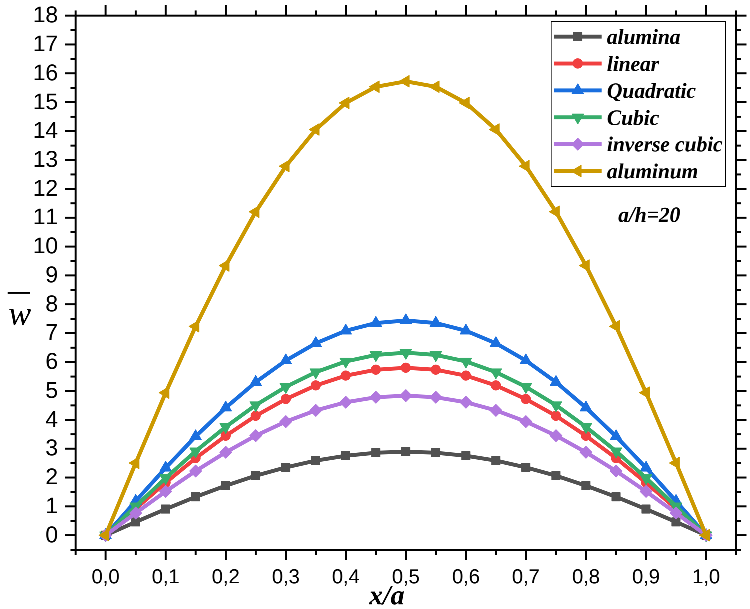

Fig 3 : Variation of the non-dimensional deflection along the plate length direction (*a/h* =20) of beams with deferent volume-fraction Vc

Fig 2 shows the normalized transverse displacement ($\bar{w}$) as a function of the span-to-depth ratio (*a/h*) for functionally graded beams with different compositional profiles (*Vc*). The results illustrate that the center deflection of FG beams is greater than that of fully ceramic (Al_2O_3) beams but less than that of fully metallic (Al) beams. The center deflection ($\bar{w}$) follows a quadratic trend for the compositional profiles, which is greater than the deflections for linear, cubic, and inverse quadratic profiles. Notably, the inverse quadratic profile results in smaller deflections than the linear and cubic profiles, while the linear profile leads to smaller deflections than the cubic profile.

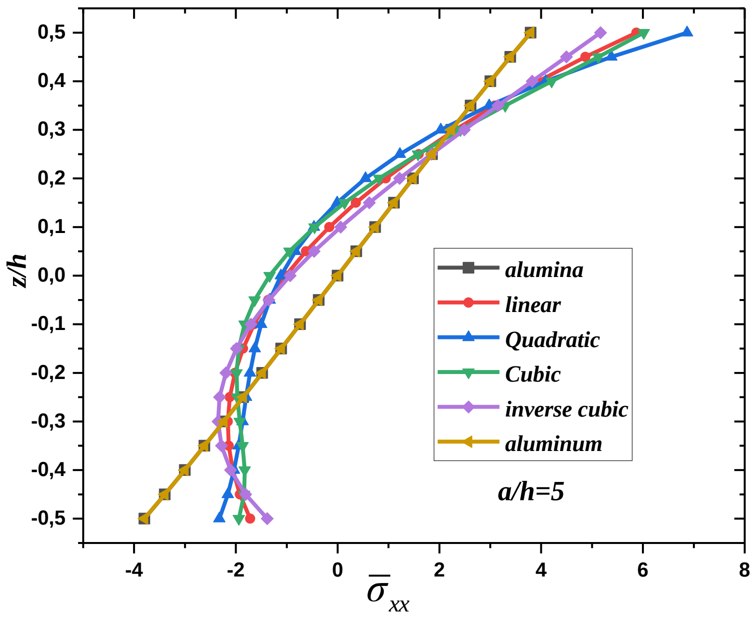

Fig 4.a : Variation of the non-dimensional normal stress $\overline{\sigma}_{xx}$ through the thickness (a/h =5) of square plate using: different volume-fraction Vc.

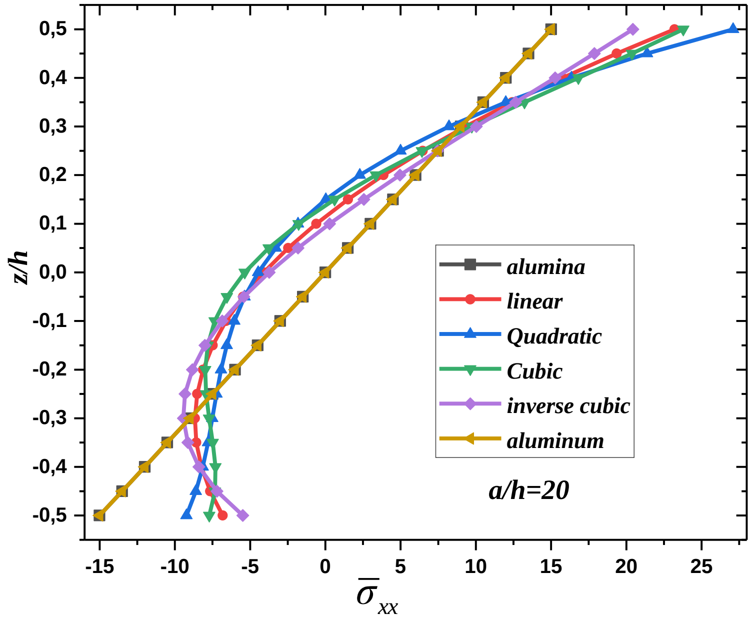

Fig 4.b : Variation of the non-dimensional normal stress $\overline{\sigma}_{xx}$ through the thickness (a/h =20) of square plate using: different volume-fraction Vc.

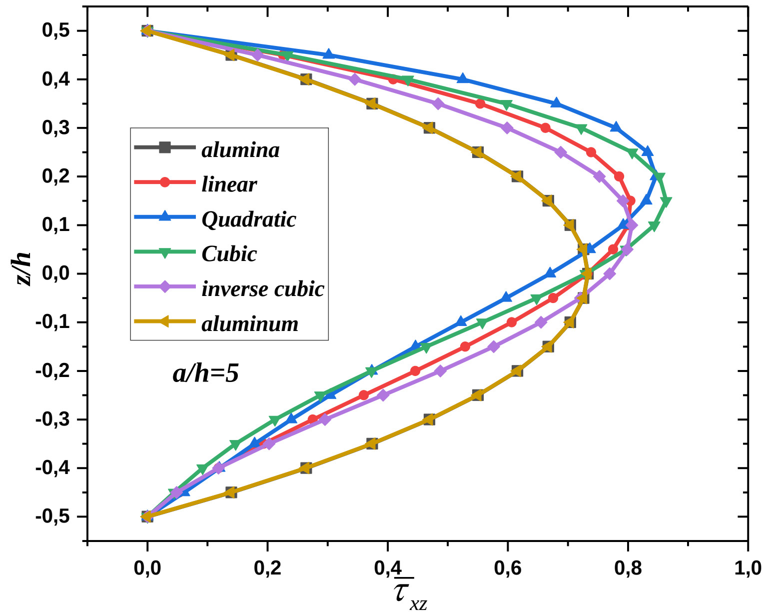

Fig 5.a: Variation of the non-dimensional transverse shear stress $\bar{\tau}_{xz}$ through the thickness (a/h =5) of square plate using: deferent volume-fraction Vc.

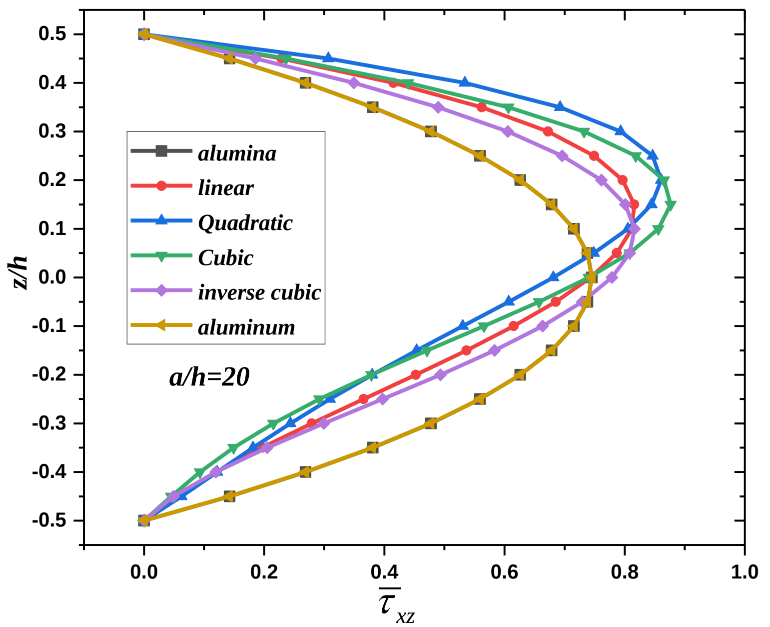

Fig 5.b: Variation of the non-dimensional transverse shear stress $\bar{\tau}_{xz}$ through the thickness (a/h =20) of square plate using: deferent volume-fraction Vc.

Fig.3 depicts the variation of non-dimensional transversal displacement ($\bar{w}$) in relation to non-dimensional length for different compositional profiles (Vc). Furthermore, it is noteworthy that the deflections for ceramic (Al2O3)-rich beams are lower than those for metal-rich (aluminum) beams.

In Fig.4a and 4b, the axial stress distribution is illustrated, showcasing a compressive stress at the bottom surface and tensile stress at the top surface of Functionally Graded (FG) plates. The extreme conditions of a homogeneous ceramic (alumina) plate (k = 0) or a metal (aluminum) plate ($k \rightarrow \infty$) result in maximum tensile axial stress at the bottom surface and minimum compressive axial stress at the top surface of the FG plate.

Fig.5a and 5b present the variation of transverse shear stress across the thickness of square homogeneous and FG plates, incorporating linear, quadratic, cubic, and inverse quadratic profiles, respectively. The through-the-thickness distributions of transverse shear stresses for FG beams with linear, quadratic, cubic, and inverse quadratic compositional profiles (Vc) deviate from the parabolic pattern observed in homogeneous metal or ceramic beams. Fig.5a and 5b underscore the substantial impact of different volume fractions of constituent materials on transverse shear stresses throughout the plate thickness, with shear stress values being notably higher in cases of volume fractions exhibiting cubic profiles (Vc).

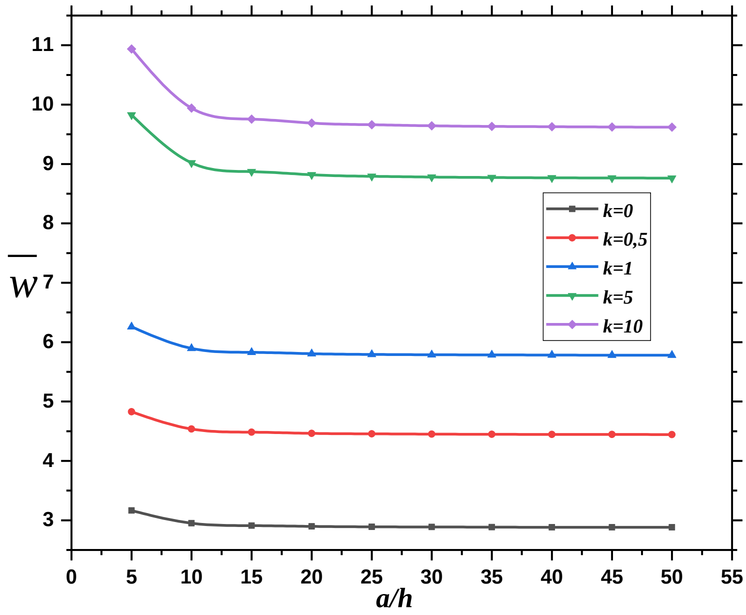

Fig 6 : variation of the non-dimensional deflection of the FGM beams versus side-to-thickness ratio (a/h) for different values of the index k.

Fig.6 illustrates the relationship between the non-dimensional deflection of FG beams and the side-to-thickness ratio (a/h), considering various values of the index k. The trend reveals that the non-dimensional deflection ($\bar{w}$) of FGM beams decreases as the ratio a/h increases and increases with a reduction in the power law index (k).

Furthermore, it is evident that the deflection of metal-rich FG beams surpasses that of ceramic-rich FG beams. This discrepancy can be attributed to the higher Young's modulus of ceramics (380 GPa) compared to that of metals (70 GPa).

The next section explores the impact of different boundary conditions simply supported (SS), clamped-clamped (CC), and clamped-free (CF) on the non-dimensional deflection of FG beams in relation to the power law index k (with aspect ratios l/h equal to 5 and 20).

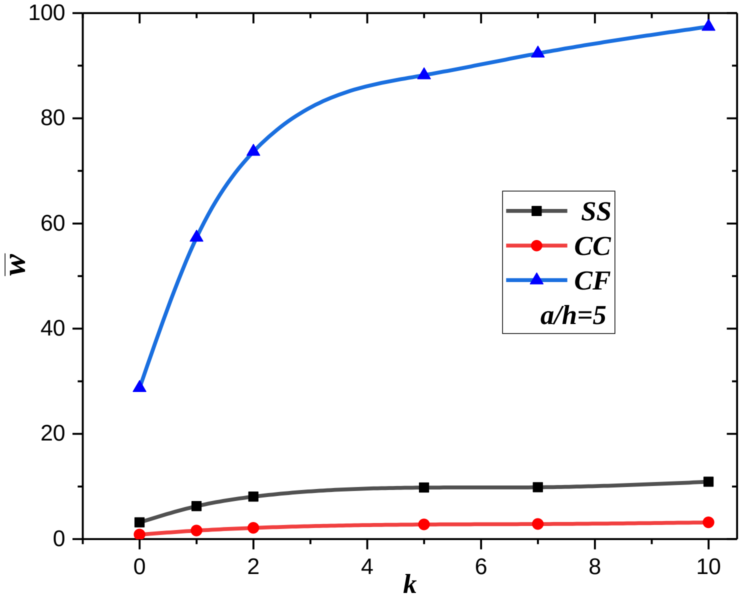

Fig 7 : variation of the non-dimensional deflection of the FG beams versus power law index k for different boundary conditions : SS,CC,CF (l/h=5).

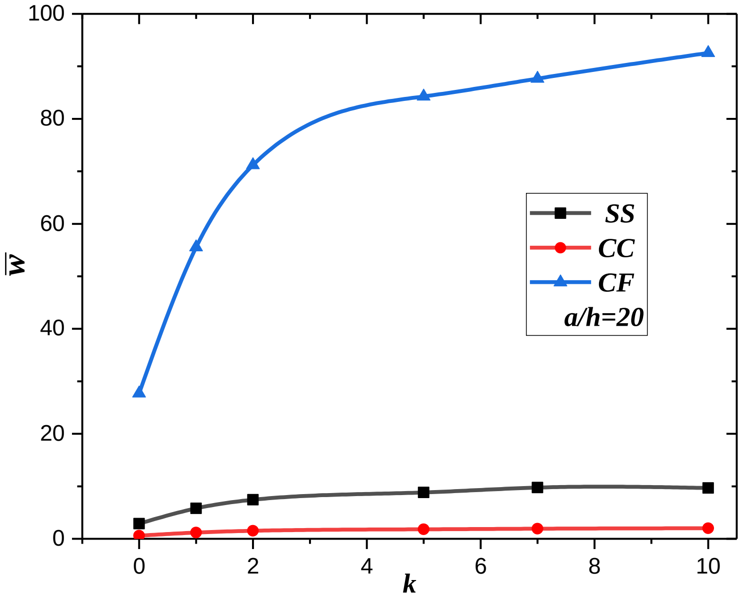

Fig 8 : variation of the non-dimensional deflection of the FG beams versus power law index k for different boundary conditions: SS,CC,CF (l/h=20).

In Fig.7 and 8, a comprehensive examination of the non-dimensional deflection of Functionally Graded (FG) beams is presented in relation to the power law index (k), considering distinct boundary conditions. Specifically, the variations in deflection are scrutinized for three specific boundary conditions: simply supported (SS), clamped-clamped (CC), and clamped-free (CF). The aspect ratio is maintained at l/h=5 in Figure 7 and l/h=20 in Figure 8.

Within Fig.7 and 8, the non-dimensional maximum deflections of beams as the power law index (k) increases. An escalation in k implies an augmentation in ceramic content, leading to heightened beam stiffness and subsequently increased non-dimensional maximum deflections.

7. Conclusion

This study has systematically explored the bending behavior of functionally graded (FG) beams by employing an original 2D refined shear deformation theory. Comprehensive comparative and parametric analyses were meticulously conducted to not only validate the proposed approach but also elucidate the intricate influences of material composition on the structural response.

The findings unequivocally established a commendable agreement with existing analytical solutions, thereby affirming the accuracy and reliability of the refined 2D theory utilized in this research. The parametric studies uncovered pivotal trends, including the central deflection of FG beams falling between those of fully ceramic and fully metallic beams. Noteworthy variations were observed with quadratic compositional gradation, resulting in higher deflections compared to linear, cubic, or inverse profiles. Axial stress distributions ranged from compressive at the bottom to tensile at the top, reaching maxima for homogeneous ceramic or metal configurations. Additionally, the shear stress distributions for FG beams exhibited a notable departure from the parabolic shape characteristic of homogeneous beams.

In essence, the refined 2D theory has not only offered valuable insights into the intricate relationship between composition profiles and displacement and stress fields in FG beams but has also paved the way for optimizing stiffness and strength through judicious material gradation. Future endeavors could extend the application of this analytical framework to explore additional gradient configurations, diverse loading scenarios, and various boundary conditions. The prospect of coupling the mechanics solutions with optimization methods holds promise for the design and engineering of high-performance Functionally Graded Material (FGM) structural components.

References

[1] V. Birman, L. W. Byrd, Modeling and analysis of functionally graded materials and structures, 2007.

[2] M. Koizumi, Functionally gradient materials the concept of FGM, *Ceramic transactions,* Vol. 34, pp. 3-10, 1993.

[3] E. Mueller, Č. Drašar, J. Schilz, W. Kaysser, Functionally graded materials for sensor and energy applications, *Materials Science and Engineering: A,* Vol. 362, No. 1-2, pp. 17-39, 2003.

[4] H.-S. Shen, Nonlinear bending response of functionally graded plates subjected to transverse loads and in thermal environments, *International Journal of Mechanical Sciences,* Vol. 44, No. 3, pp. 561-584, 2002.

[5] B. V. Sankar, An elasticity solution for functionally graded beams, *Composites Science and Technology,* Vol. 61, No. 5, pp. 689-696, 2001.

[6] Z. Zhong, T. Yu, Analytical solution of a cantilever functionally graded beam, *Composites Science and Technology,* Vol. 67, No. 3-4, pp. 481-488, 2007.

[7] R. Kadoli, K. Akhtar, N. Ganesan, Static analysis of functionally graded beams using higher order shear deformation theory, *Applied mathematical modelling,* Vol. 32, No. 12, pp. 2509-2525, 2008.

[8] M. Benatta, I. Mechab, A. Tounsi, E. A. Bedia, Static analysis of functionally graded short beams including warping and shear deformation effects, *Computational Materials Science,* Vol. 44, No. 2, pp. 765-773, 2008.

[9] X.-F. Li, B.-L. Wang, J.-C. Han, A higher-order theory for static and dynamic analyses of functionally graded beams, *Archive of Applied Mechanics,* Vol. 80, pp. 1197-1212, 2010.

[10] T. P. Vo, H.-T. Thai, T.-K. Nguyen, F. Inam, J. Lee, Static behaviour of functionally graded sandwich beams using a quasi-3D theory, *Composites Part B: Engineering,* Vol. 68, pp. 59-74, 2015.

[11] M. Bourada, A. Kaci, M. S. A. Houari, A. Tounsi, A new simple shear and normal deformations theory for functionally graded beams, *Steel Compos. Struct,* Vol. 18, No. 2, pp. 409-423, 2015.

[12] H.-T. Thai, T. P. Vo, Bending and free vibration of functionally graded beams using various higher-order shear deformation beam theories, *International journal of mechanical sciences,* Vol. 62, No. 1, pp. 57-66, 2012.

[13] G. Giunta, D. Crisafulli, S. Belouettar, E. Carrera, A thermo-mechanical analysis of functionally graded beams via hierarchical modelling, *Composite Structures,* Vol. 95, pp. 676-690, 2013.

[14] S. S. Pendhari, T. Kant, Y. M. Desai, C. Venkata Subbaiah, On deformation of functionally graded narrow beams under transverse loads, *International Journal of Mechanics and Materials in Design,* Vol. 6, pp. 269-282, 2010.

[15] A. Arbind, J. Reddy, A. Srinivasa, Modified couple stress-based third-order theory for nonlinear analysis of functionally graded beams, *Latin American journal of solids and structures,* Vol. 11, pp. 459-487, 2014.

[16] L. Ma, D. Lee, A further discussion of nonlinear mechanical behavior for FGM beams under in-plane thermal loading, *Composite Structures,* Vol. 93, No. 2, pp. 831-842, 2011.

[17] S. Esfahani, Y. Kiani, M. Eslami, Non-linear thermal stability analysis of temperature dependent FGM beams supported on non-linear hardening elastic foundations, *International Journal of Mechanical Sciences,* Vol. 69, pp. 10-20, 2013.
[18] H.-S. Shen, Postbuckling analysis of axially-loaded functionally graded cylindrical shells in thermal environments, *Composites Science and Technology,* Vol. 62, No. 7-8, pp. 977-987, 2002.
[19] M. Filippi, E. Carrera, A. Zenkour, Static analyses of FGM beams by various theories and finite elements, *Composites Part B: Engineering,* Vol. 72, pp. 1-9, 2015.
[20] A. Chakraborty, S. Gopalakrishnan, J. Reddy, A new beam finite element for the analysis of functionally graded materials, *International journal of mechanical sciences,* Vol. 45, No. 3, pp. 519-539, 2003.
[21] J. H. Kim, G. H. Paulino, Finite element evaluation of mixed mode stress intensity factors in functionally graded materials, *International Journal for Numerical Methods in Engineering,* Vol. 53, No. 8, pp. 1903-1935, 2002.
[22] L. Sator, V. Sladek, J. Sladek, Bending of FGM plates under thermal load: classical thermoelasticity analysis by a meshless method, *Composites Part B: Engineering,* Vol. 146, pp. 176-188, 2018.
[23] J. C. H. B.L. Wang, S.Y. Du, , A differential quadrature treatment of bending problems of functionally graded beams, *Mechanics of Advanced Materials and Structures,* Vol. 8, No. 2, pp. 135-144,
2001.
[24] V. Kahya, M. Turan, Finite element model for vibration and buckling of functionally graded beams based on the first-order shear deformation theory, *Composites Part B: Engineering,* Vol. 109, pp. 108-115, 2017.
[25] A. Frikha, A. Hajlaoui, M. Wali, F. Dammak, A new higher order C0 mixed beam element for FGM beams analysis, *Composites Part B: Engineering,* Vol. 106, pp. 181-189, 2016.
[26] J. Aboudi, Micromechanical analysis of fully coupled electro-magneto-thermo-elastic multiphase composites, *Smart materials and structures,* Vol. 10, No. 5, pp. 867, 2001.
[27] G. Giunta, S. Belouettar, E. Carrera, Analysis of FGM beams by means of classical and advanced theories, *Mechanics of Advanced Materials and Structures,* Vol. 17, No. 8, pp. 622-635, 2010.
[28] A. S. Sayyad, Y. M. Ghugal, Bending, buckling and free vibration of laminated composite and sandwich beams: A critical review of literature, *Composite Structures,* Vol. 171, pp. 486-504, 2017.
[29] A. S. Sayyad, Y. M. Ghugal, Analytical solutions for bending, buckling, and vibration analyses of exponential functionally graded higher order beams, *Asian Journal of Civil Engineering,* Vol. 19, pp. 607-623, 2018.
[30] S. Mohanty, R. Dash, T. Rout, Static and dynamic stability analysis of a functionally graded Timoshenko beam, *International Journal of Structural Stability and Dynamics,* Vol. 12, No. 04, pp. 1250025, 2012.
[31] S.-R. Li, R. C. Batra, Relations between buckling loads of functionally graded Timoshenko and homogeneous Euler–Bernoulli beams, *Composite Structures,* Vol. 95, pp. 5-9, 2013.
[32] R. Benferhat, T. H. Daouadji, M. S. Mansour, Free vibration analysis of FG plates resting on an elastic foundation and based on the neutral surface concept using higher-order shear deformation theory, *Comptes Rendus Mecanique,* Vol. 344, No. 9, pp. 631-641, 2016.
[33] A. Berkia, B. Rebai, B. Litouche, S. Abbas, K. Mansouri, Investigating parametric homogenization models for natural frequency of FGM nano beams, *AIMS Materials Science,* Vol. 10, No. 5, 2023.
[34] R. Billel, Effect of the Idealization Models and Thermal Loads on Deflection Behavior of Sandwich FGM Plate, in *Proceeding of,* IEEE, pp. 260-264.
[35] R. Billel, Contribution to study the effect of (Reuss, LRVE, Tamura) models on the axial and shear stress of sandwich FGM plate (Ti-6A1-4V/ZrO 2) subjected on linear and nonlinear thermal loads, *AIMS Materials Science,* Vol. 10, No. 1, 2023.
[36] Y. Xu, T. Yu, D. Zhou, Two-dimensional elasticity solution for bending of functionally graded beams with variable thickness, *Meccanica,* Vol. 49, pp. 2479-2489, 2014.
[37] B. Rebai, K. Mansouri, M. Chitour, A. Berkia, T. Messas, F. Khadraoui, B. Litouche, Effect of Idealization Models on Deflection of Functionally Graded Material (FGM) Plate, 2023.
[38] A. Boussoula, B. Boucham, M. Bourada, F. Bourada, A. Tounsi, A. A. Bousahla, A. Tounsi, A simple nth-order shear deformation theory for thermomechanical bending analysis of different configurations of FG sandwich plates, *Smart Structures and Systems, An International Journal,* Vol. 25, No. 2, pp. 197-218, 2020.
[39] J. Aboudi, S. M. Arnold, M.-J. Pindera, Response of functionally graded composites to thermal gradients, *Composites Engineering,* Vol. 4, No. 1, pp. 1-18, 1994.
[40] S. Esfahani, Y. Kiani, M. Komijani, M. Eslami, Vibration of a temperature-dependent thermally pre/postbuckled FGM beam over a nonlinear hardening elastic foundation, *Journal of Applied Mechanics,* Vol. 81, No. 1, pp. 011004, 2014.

[41] R. Kolahchi, S.-P. Zhu, B. Keshtegar, N.-T. Trung, Dynamic buckling optimization of laminated aircraft conical shells with hybrid nanocomposite martial, *Aerospace Science and Technology,* Vol. 98, pp. 105656, 2020.
[42] B. Keshtegar, A. Farrokhian, R. Kolahchi, N.-T. Trung, Dynamic stability response of truncated nanocomposite conical shell with magnetostrictive face sheets utilizing higher order theory of sandwich panels, *European Journal of Mechanics-A/Solids,* Vol. 82, pp. 104010, 2020.
[43] B. Keshtegar, M. Motezaker, R. Kolahchi, N.-T. Trung, Wave propagation and vibration responses in porous smart nanocomposite sandwich beam resting on Kerr foundation considering structural damping, *Thin-Walled Structures,* Vol. 154, pp. 106820, 2020.
[44] H. Golabchi, R. Kolahchi, M. R. Bidgoli, Vibration and instability analysis of pipes reinforced by SiO2 nanoparticles considering agglomeration effects, *Computers and Concrete, An International Journal,* Vol. 21, No. 4, pp. 431-440, 2018.
[45] M. H. Hajmohammad, M. Maleki, R. Kolahchi, Seismic response of underwater concrete pipes conveying fluid covered with nano-fiber reinforced polymer layer, *Soil Dynamics and Earthquake Engineering,* Vol. 110, pp. 18-27, 2018.
[46] M. Al-Furjan, A. Farrokhian, B. Keshtegar, R. Kolahchi, N.-T. Trung, Higher order nonlocal viscoelastic strain gradient theory for dynamic buckling analysis of carbon nanocones, *Aerospace Science and Technology,* Vol. 107, pp. 106259, 2020.
[47] M. Al-Furjan, A. Farrokhian, S. Mahmoud, R. Kolahchi, Dynamic deflection and contact force histories of graphene platelets reinforced conical shell integrated with magnetostrictive layers subjected to low-velocity impact, *Thin-Walled Structures,* Vol. 163, pp. 107706, 2021.
[48] M. H. Hajmohammad, A. H. Nouri, M. S. Zarei, R. Kolahchi, A new numerical approach and visco-refined zigzag theory for blast analysis of auxetic honeycomb plates integrated by multiphase nanocomposite facesheets in hygrothermal environment, *Engineering with Computers,* Vol. 35, pp. 1141-1157, 2019.
[49] R. Kolahchi, F. Kolahdouzan, A numerical method for magneto-hygro-thermal dynamic stability analysis of defective quadrilateral graphene sheets using higher order nonlocal strain gradient theory with different movable boundary conditions, *Applied Mathematical Modelling,* Vol. 91, pp. 458-475, 2021.
[50] M. H. Hajmohammad, M. B. Azizkhani, R. Kolahchi, Multiphase nanocomposite viscoelastic laminated conical shells subjected to magneto-hygrothermal loads: Dynamic buckling analysis, *International Journal of Mechanical Sciences,* Vol. 137, pp. 205-213, 2018.
[51] M. Chitour, A. Bouhadra, M. Benguediab, K. Mansouri, A. Menasria, A. Tounsi, A New High Order Theory for Buckling Temperature Analysis of Functionally Graded Sandwich Plates Resting on Elastic Foundations, *Journal of Nano-and Electronic Physics,* Vol. 14, No. 3, 2022.
[52] L. O. Larbi, A. Kaci, M. S. A. Houari, A. Tounsi, An efficient shear deformation beam theory based on neutral surface position for bending and free vibration of functionally graded beams#, *Mechanics Based Design of Structures and Machines,* Vol. 41, No. 4, pp. 421-433, 2013.
[53] M. Chitour, A. Bouhadra, M. Benguediab, K. Mansouri, A. Menasria, A. Tounsi, A New High Order Theory for Buckling Temperature Analysis of Functionally Graded Sandwich Plates Resting on Elastic Foundations, 2022.